Available online at www.sciencedirect.com
ScienceDirect
Computers and Geotechnics 35 (2008) 305–308
COMPUTERS AND GEOTECHNICS
www.elsevier.com/locate/compgeo

Comments on 'Two-dimensional slope stability analysis by limit equilibrium and strength reduction methods' by Y.M. Cheng, T. Lansivaara and W.B. Wei [Computers and Geotechnics 34 (2007) 137–150]

J. Bojorque *, G. De Roeck, J. Maertens

Department of Civil Engineering, Katholieke Universiteit Leuven, Kasteelpark Arenberg 40, B-3001 Leuven, Belgium

Received 18 April 2007
Available online 11 June 2007

In the first part of the paper the authors present a comparative analysis between the location of the critical sliding surface computed by limit equilibrium method (LEM) using an optimization procedure (annealing technique) and the location of the maximum shear strains (total/incremental) computed by finite element analysis (FE) determined from the strength reduction method (SRM). For the FE-SRM both non-associated flow rule (SRM1) and associated (SRM2) are used. Furthermore, in this section the authors present a comparison between the factor of safety values (FOS) computed by Spencer's method and the SRM1 and SRM2. Next, the authors have constructed three interesting cases where the applicability of SRM *might* be limited. The first example presents the influence of a soft band in SRM. In the two other examples the presence of different sliding surfaces is highlighted. In the last section a small parametric study with respect to the influence of the elastic modulus for SRM is presented.

1. Comparative analysis between LEM and FE-SRM

The authors conclude from the first part that for most of the cases the FOS obtained by SRM are slightly larger than those obtained by LEM with only few exceptions. However, by performing a FE-SRM with PLAXIS (commercial finite element package) [1], the discussers found that for all of the cases the FOS values are lower than those obtained by the authors' method, and for most of the cases slightly lower than LEM.

It is worth mentioning that the FOS computed from Spencer's method without optimization procedure (annealing technique) are higher than SRM. However, for some cases (especially case 16 and other cases with low friction angle) using the optimization technique, the FOS value might be 10% lower than SRM, and for those cases the location of the sliding surface differs. These cases should be considered for further analysis.

It is assumed that the authors performed the FE-SRM calculations for a maximum tensile strength equal to the cohesion divided by the tangent of the friction angle, related to Mohr–Coulomb failure criteria. Most of the soils do not support or support small tensile strength and a tension-cut off equal to zero, i.e. tensile strength equal to zero, is more realistic and conservative. To extend the comparative analysis, a tension-cut off for both non-associated flow rule (SRM1T) and associated (SRM2T) has been introduced. The presence or absence of a tension-cut off influences the computation of the factor of safety in SRM and at the same time affects the location of the sliding surface especially at the crest of the slope. Moreover, the tension-cut off might cause concentration of strains at the toe of the slope for a associated flow rule. For this case, the determination of the sliding surface derived from the total/incremental shear strain contours needs extra care.

Table 1 present the comparative analysis using PLAXIS with and without the inclusion of the tension-cut off. Based on Table 1 some summary conclusions can be made as follows:

* Corresponding author.
E-mail address: jaime.bojorque@bwk.kuleuven.be (J. Bojorque).

doi:10.1016/j.compgeo.2007.04.005

Table 1
Factor of safety (FOS) by LEM and SRM

1	2	3	4	5/6	7/8	9/10	11/12	13/14	15/16
Case	c' (kPa)	ϕ' (°)	FOS (LEM)	Cheng et al. (SRM1/SRM2)	Plaxis (SRM1/SRM2)	%Plaxis-LEM (SRM1/SRM2)	%Plaxis-Cheng (SRM1/SRM2)	Plaxis(Tension-cut) (SRM1T/SRM2T)	%Plaxis(T)-LEM (SRM1T/SRM2T)
1	2	5	0.25	0.25/0.26	0.25/0.25	−1.00/0.9	−1.00/−3.0	0.24/0.25	−5.5/−1.3
2	2	15	0.50	0.51/0.52	0.45/0.50	−10.3/−0.6	−12.1/−4.4	0.46/0.49	−9.0/−1.9
3	2	25	0.74	0.77/0.78	0.66/0.75	−11.2/1.0	−14.6/−4.2	0.65/0.75	−12.4/0.9
4	2	35	1.01	1.07/1.07	0.92/1.03	−8.60/2.0	−13.7/−3.8	0.85/1.02	−15.5/1.4
5	2	45	1.35	1.42/1.44	1.11/1.35	−17.4/0.1	−21.5/−6.2	1.24/1.25	−8.4/−7.7
6	5	5	0.41	0.43/0.43	0.42/0.42	2.5/3.2	−2.3/−1.6	0.41/0.41	−0.7/0.0
7	5	15	0.70	0.73/0.73	0.69/0.71	−1.9/1.6	−6.0/−2.6	0.67/0.69	−3.9/−1.7
8	5	25	0.98	1.03/1.03	0.90/0.99	−7.8/1.4	−12.3/−3.5	0.89/0.97	−8.8/−1.5
9	5	35	1.28	1.34/1.35	1.16/1.29	−9.1/0.8	−13.2/−4.5	1.14/1.28	−11.1/−0.3
10	5	45	1.65	1.68/1.74	1.45/1.62	−11.9/−2.1	−13.5/−7.1	1.45/1.61	−11.9/−2.6
11	10	5	0.65	0.69/0.69	0.68/0.68	4.6/4.8	−1.4/−1.3	0.65/0.65	0.3/0.4
12	10	15	0.98	1.04/1.04	0.99/1.01	1.2/2.7	−4.7/−3.2	0.97/0.98	−1.1/0.3
13	10	25	1.30	1.36/1.37	1.27/1.32	−2.2/1.2	−6.5/−4.0	1.24/1.29	−4.8/−0.9
14	10	35	1.63	1.69/1.71	1.56/1.63	−4.3/0.0	−7.7/−4.7	1.51/1.60	−7.3/−1.7
15	10	45	2.04	2.05/2.15	1.89/1.97	−7.6/−3.5	−8.0/−8.5	1.84/1.96	−9.7/−4.0
16	20	5	1.06	1.20/1.20	1.17/1.17	10.7/10.7	−2.2/−2.3	1.12/1.12	5.5/5.5
16[a]	20	5	1.19		1.17/1.17	−1.4/−1.4			
17	20	15	1.48	1.59/1.59	1.54/1.53	4.0/3.5	−3.2/−3.7	1.48/1.49	0.0/0.4
18	20	25	1.85	1.95/1.96	1.87/1.87	1.2/1.3	−4.0/−4.4	1.81/1.82	−1.9/−1.5
19	20	35	2.24	2.28/2.35	2.23/2.20	−0.5/−1.9	−2.3/−6.5	2.15/2.14	−3.8/−4.3
20	20	45	2.69	2.67/2.83	2.62/2.55	−2.8/−5.2	−2.0/−9.9	2.56/2.49	−4.9/−7.3
21[b]	5	0	0.20	–/0.23	–/0.22	–/11.1	–/−3.4	–/0.22	–/7.9
22[b]	10	0	0.40	–/0.45	–/0.44	–/11.1	–/−1.3	–/0.43	–/7.6
23[b]	20	0	0.80	–/0.91	–/0.89	–/11.1	–/−2.3	–/0.87	–/8.7

[a] Slip surface without optimization.
[b] Critical slip surface located infinitely deep.

(1) For all cases PLAXIS computed FOS that are lower than the authors' values. The differences range from 1% to 21.5%. The differences might be attributed to the type of nonlinear solution algorithm.
(2) In contrary to the authors' statement one, most of the FOS obtained from the SRM1 are smaller than those obtained from the LEM with only few exceptions (some optimization cases). These differences increase when zero-tensile strength is introduced. LEM with optimization search computed FOS values lower than SRM1 when the friction angle is small.
(3) In general the FOS when using an associated flow rule (SRM2) and (SRM2T) are slightly greater than those from a non-associated flow (SRM1) and (SRM1T), respectively. Exceptions are cases 19 and 20 where this relation changes.
(4) When the cohesion of the soil is higher than 5 kPa and the tensile strength is neglected, the differences are greatest for higher friction angles (column 15 Table 1).
(5) For the cases where $\phi = 0°$, SRM produced a very deep seated slip surface affected by the boundaries. For these cases (21–23) the FOS computed for SRM are not representative for the most unfavourable situation. Any comparative analysis between the FOS and the location of the sliding surface according to LEM and SRM should take into account this condition.

Another important aspect that should be considered is the initial state of stress (ISS) used to perform SRM. Stresses measured in the field are almost never available, and for cases where the FOS is expected to be higher than 1 (stable slope), the gravity loading procedure is appropriate to evaluate the ISS. However, for cases where FOS < 1 (unstable slope), the gravity loading procedure fails to reach the whole weight. For these cases the computation of ISS could be replaced by a K_0 procedure, where $K_0 = \sigma_x/\sigma_y$. The computation of the ISS might affect the FOS and the location of the critical sliding surface.

In this section some remarks are given that need authors' consideration:

(a) For the examples depicted in Fig. 5 and cases 21–23 (Table 1), where $\phi = 0°$ and slope inclination $\beta \leqslant 53°$, the location of the critical slip surface is expected to be infinitely deep (Taylor chart 1948). From performing the FE-SRM, this situation is clear from the fact that the boundaries affect the location of the slip surface and extending the boundaries as done by the authors, or even further, does not help to determine the critical location of the sliding surface. LEM always detect the *worst* surface (might or might not be the critical surface) within the range of the search input parameters (search grid, search radius, entry and exit points, and so on).

(b) Information on the characteristics of the numerical method, solution algorithm and computation of the initial state of stresses, in the authors' analyses might be helpful in understanding the differences.
(c) For further studies, it could be helpful to provide the procedure used to define the critical sliding line from the shear strain contours used by the authors. Although, the authors' interest is mainly on the location of the critical sliding surface, the statements regarding the FOS should be reevaluated as well.
(d) The authors mentioned on p. 2 that there are limited studies which compare the critical failure surfaces from LEM and SRM. For further studies, it could be helpful to provide the references and the conclusions of these limited studies.

2. Other failure surface by FE-SRM

The authors state that "It is possible that the use of the SRM may miss the location of the next critical failure surface (with a very small difference in the FOS but a major difference in the location of the critical failure surface) so that the slope stabilization measures may not be adequate. This interesting case has illustrated a major limitation of the SRM for the design of slope stabilization works."

The study made by Cala et al. [2] presents the use of numerical techniques for determining other failure surfaces apart form the critical one. A modified shear strength reduction technique (MSSR) is applied which is based on reducing the shear strength properties of soils after identification of the first slip surface. The benched slope used in [2] is similar to the example depicted by the authors in Fig. 13. The method proposed by Cala et al. needs extra computations and is also applicable to the case of unstable slopes FOS < 1, which may cause some numerical problems in FE-SRM.

Based on their experience working with FE-SRM, the discussers present a procedure to deal with the location of other failure surfaces by retaining all the steps in the SRM computations and without the need of extra computations. Further research is still going on, but the possibility to capture different sliding surfaces apart from the critical one by performing FE-SRM seems to be possible as illustrated by the next examples. Moreover, the representation by a single line to characterize the sliding mechanism can be misleading for the implementation of remedial measures. And the advantage of FE-SRM in getting a sliding zone (shear strain contours) is lost by trying to extract a single line from these zones.

The same criteria as used by Renaud et al. [3] in LEM are used. In the paper, the necessity to retain and visualize *all* slip surface information to determine the full extent of potential slope instability is mentioned. All steps in FE-SRM (different strength reduction computations) are retained and all possible unstable mechanics checked to determine the full potential zones of instability.

Comparative analyses are presented for the examples given by the authors and additional safety maps are presented following the procedure given by Renaud et al. [3]. The safety map is constructed by minimizing the factor of safety between all the slip surfaces going through a mesh point. The slope is discretized and for each point in the mesh the minimum FOS value that is near to the point is assigned. A rectangular mesh spacing of 0.20 m is used for the discretization, and for each node the selection of the slip circles (Bishop) that intersect a rectangle of length 0.20 m was used. A filtering FOS value of 1.6 was used for visualization purpose. The result is a safety map where the

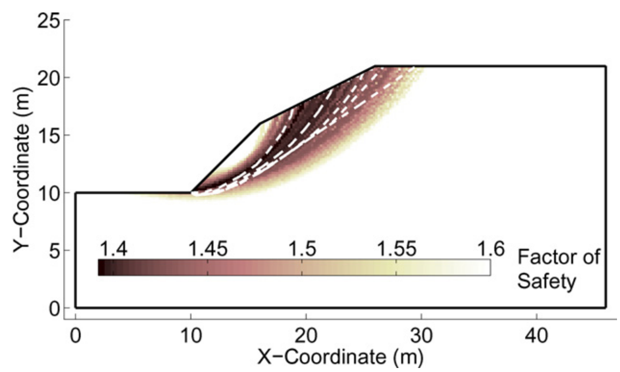

Fig. 19. Safety map by LEM, example 1.

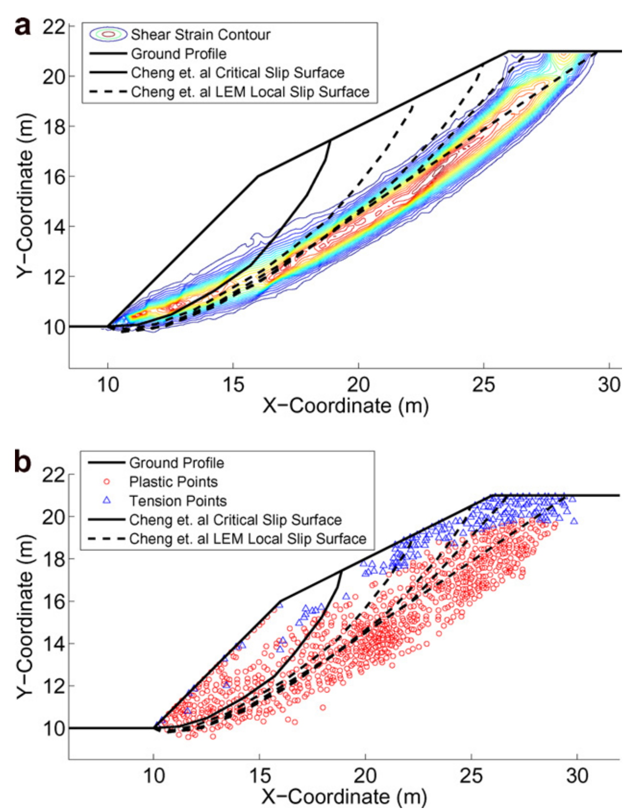

Fig. 20. Critical zones by FE-SRM, example 1. (a) Incremental shear strain contours and (b) Plastic points.

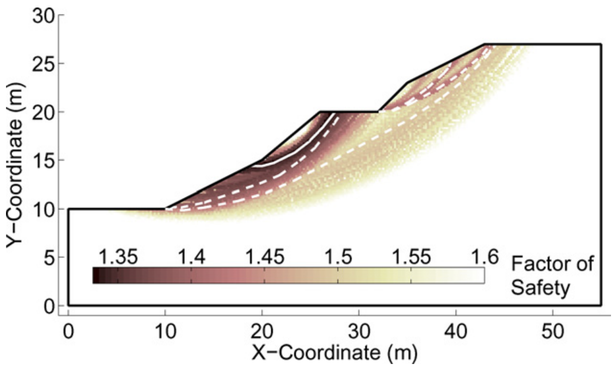

Fig. 21. Safety map by LEM, example 2.

different FOS are depicted. More details about the procedure is presented in [3].

The two slope angles example presented by the authors in Figs. 10–12 is less critical because the potential sliding mechanism falls inside the shear zone computed from FE-SRM. Any slope stabilization measure done for the most critical failure mechanism will affect the other mechanisms. Soil parameter $c = 10$ kPa, $\phi = 30°$, $\psi = 0°$ and zero-tensile strength are used. The safety map computed using the aforementioned procedure is shown in Fig. 19, in which the visualization of the local minima is better than when presenting few sliding lines. The limit equilibrium sliding surfaces obtained by the authors are superimposed. This safety map is important for the design and implementation of stabilization actions.

Shear strain contours and plastic zones developed by the FE-SRM are shown in Fig. 20. In this case, the FE-SRM procedure capture all the potential sliding surfaces and the implementation of any remedial measure will fall in this zone.

The case presented in Fig. 13 needs the retention and visualization of the whole SRM. The FOS computed in PLAXIS for this case is 1.302 in which $c = 5$ kPa, $\phi = 30°$, $\psi = 0°$ and zero-tensile strength are used. The critical sliding surface is similar to Fig. 13f, in which only the global minimum is detected. The safety map in which the sliding lines presented by the authors are superimposed is shown in Fig. 21. This safety map depicted all the potential unstable zones. Shear strain contours and plastic/tension points developed in a FE-SRM step are shown in Fig. 22. It is worth noticing that the SRM captures the different failure surfaces, thus retaining the information given in the different FE-SRM steps helps to the design and the implementation of stabilization actions. From these figures the zone of instability can be clearly detected. The good representation of all the possible sliding surfaces makes it plausible to use FE-SRM to detect multiple failure mechanism.

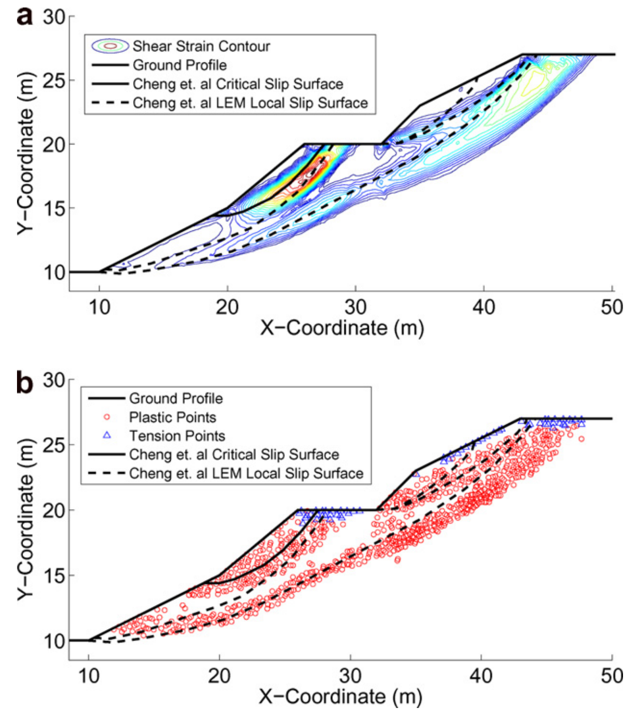

Fig. 22. Critical zones by FE-SRM, example 2. (a) Incremental shear strain contours and (b) Plastic points.

References

[1] PLAXIS BV. Finite Element Code for Soil and Rock Analysis. Slope Stability Analysis, Delft University of Technology and Plaxis, The Netherlands; 2004.

[2] Cala M, Flisiak J, & Tajdus A. Slope stability analysis with modified shear strength reduction technique. in: Lacerda W, Erlich M, Fontoura S, Sayao A. (editors), Proceedings of the Nineth International Symposium on Landslides; Landslides: Evaluation and Stabilization, Rio de Janeiro, Brazil; 2004.

[3] Renaud J-P, Anderson M, Wilkinson P, Lloyd D, Muir-Wood D. The importance of visualisation of results from slope stability analysis. Proc ICE Geotech Eng 2003;156:27–33.